Applied Radiation and Isotopes 165 (2020) 109307

Contents lists available at ScienceDirect

Applied Radiation and Isotopes

journal homepage: http://www.elsevier.com/locate/apradiso

New core configuration for the fabrication of ^{125}I radioactive sources for cancer treatment

Carla Daruich de Souza *, Carlos Alberto Zeituni, Anselmo Feher, João Augusto Moura, Osvaldo Luiz da Costa, Lucas Verdi Angelocci, Maria Elisa C.M. Rostelato

Instituto de Pesquisas Energéticas e Nucleares, Cidade Universitária, Avenida Professor Lineu Prestes, 2242 Zip-code: 05508-000, São Paulo, SP, Brazil

ARTICLE INFO

Keywords:
Iodine-125 seed core
Brachytherapy
Radiation chemistry
Monte Carlo simulation

ABSTRACT

In order to provide prostate brachytherapy treatment for more Brazilian men, IPEN is building a laboratory for the manufacture of radioactive sources. The new methodology for the production of iodine-125 seeds with yield 71.7% ± 5.3%. Points of importance were evaluated/discussed: photo-sensibility, reaction vial type, the substitution for iodine-131, pH, and solution volume. The surface was analyzed by FTIR and EDS. At the end, a Monte Carlo-MCNP6 simulation was performed to evaluate the TG-43 parameters.

1. Introduction

Deaths by cancer in Brazil reached 127 thousand in 2013. The National Institute of Cancer estimated 600 thousand new cases for the next two years 2018–2019 (Ministério da Saúde. Instituto Nacional de Câncer, 2018). Among the forms of treatment available, brachytherapy is one that many times is ignored because of the high costs involved. In Brazil, it is only covered by few private hospitals, and not provided by the country free health care system. With that in mind, a multidisciplinary research group was stablished at IPEN (Nuclear and Energy Research Institute located at the University of São Paulo) a branch of the Brazilian Nuclear Energy Commission in order to developed a new iodine-125 brachytherapy source with the goal of reducing costs and broad availability.

Interstitial brachytherapy aims for a highly localized devitalization of a well-defined treatment volume, thereby avoiding damage of the surrounding non-neoplastic tissue (Russel, 2004). Brachytherapy with iodine-125 seeds can be used as a permanent implant (e.g. prostate cancer) or by temporary exposure (e.g. eye and brain cancers). The source used usually contains a core with the radioactive material and a radiological marker that is placed inside a biocompatible capsule. The source final size is 4.5 mm length and 0.8 mm in diameter. The amount of radioactive iodine varies accordingly with the different treatments. For instance, sources used for prostate cancer usually have around 29.6–22.2 MBq (0.8–0.6 mCi) and the ones used in brain brachytherapy can reach up to 1.11 GBq (30 mCi) (Cardoso et al., 2017).

Iodine-125 brachytherapy is an effective modality to deliver a high radiation dose to the prostate while minimizing effects on the adjacent organs at risk, such as the bladder and anus (Zeituni et al., 2012). For patients with low and favorable intermediate-risk prostate cancer, brachytherapy is equally effective in controlling the disease as radical prostatectomy (Goldner et al., 2012). Prostate cancer treatment with iodine-125 brachytherapy results in 95% of the patients achieving the full cure with significant lower side effects (Chodak, 2014; Souza, 2009, 2012).

The literature regarding the fabrication methods are usually protected by patents. Lawrence presented in 1965 the first report. As a core the author recommended nylon, silicon, Teflon®, and resin. For radioactive isotope, palladium-103, cesium-131, and iodine-125 were considered. Gold and tungsten were cited as radiological markers and inox and titanium as coating materials (Lawrence, 1967). Kubiatowicz published a comprehensive patent in 1982 in which he describes four variations that used chemical exchange and/or electrodeposition with a silver core to result in the desirable $Ag^{125}I$ (Kubiatowicz, 1982). Those methodologies are still used on the fabrication of the GE- Healthcare model 6711 source (Russel, 2004). Suthanthiran et al. (Suthanthiran and Lakshman, 1991) described a source that uses a mixture of polytyrosine with cellulose as a core matrix in which the iodine-125 is placed before the cure process. After the process, the iodine is sealed with Chloramine-T. This model is used by Best Medical. Cutrer (Cutrer, 1999, 2003) presented a seed that uses 4 resin spheres as a core that contains the radioactive material incorporated. Four silver or gold spheres are

* Corresponding author.
E-mail addresses: carladdsouza@yahoo.com.br, cdsouza@ipen.br (C. Daruich de Souza), czeituni@ipen.br (C. Alberto Zeituni), afeher@ipen.br (A. Feher), jamoura@ipen.br (J. Augusto Moura), olcosta@ipen.br (O. Luiz da Costa), lucasangelocci@usp.br (L.V. Angelocci), elisaros@ipen.br (M.E.C.M. Rostelato).

https://doi.org/10.1016/j.apradiso.2020.109307
Received 10 July 2019; Received in revised form 9 June 2020; Accepted 22 June 2020
Available online 20 July 2020

used as markers. The position of the sphere is directly linked to the final desired activity. This is still being used by Mentor Corp. The "TEC-DOC-1512: Production Techniques and Quality Control of Sealed Radioactive Sources of Palladium-103, Iodine-125, Iridium-192 and Ytterbium-169" (International Atomic Energy Agency, 2006) published by IAEA presents novelties by Cieszykowska et al., Mehdikhani et al., Chakrov et al., K.J. Son et al., and Benites et al. Iodine-125 core incorporation yields ranged from 53 to 99% (International Atomic Energy Agency, 2006).

This present work objectives are: to developed a new iodine-125 binding reaction directly into a silver core seeking simplicity and easy execution. This will be implemented in the new National Laboratory for Iodine-125 Sources Production. Also, a few of the issues encountered were investigated and their impact on the current new reaction accessed. Monte-Carlo simulation using the MCNP code were performed to evaluate dosimetric parameters.

2. Materials and methods

An iodine-125 brachyseed usually has a core containing iodine-125 and a radiological marker, which may be gold, silver, etc., and an outside capsule made of biocompatible material that surrounds the core, most commonly titanium or stainless steel. Details on seed welding can be found in supporting information (SI). The schematics of the iodine seed that is being produced by IPEN is shown in Fig. 1:

The silver core was purchased from the company Cenabrás already cut into small 3 mm pieces. The composition is 99.99% pure silver. However, the silver, having a high oxidation potential, forms silver oxide, Ag_2O, when in contact with air. The silver oxide has: solubility in water of 0.0025 g/100 mL, and highly stable cubic geometry (Mellor, 1965). Thus, for the reaction to occur, surface modification is necessary either by etching or deposition that will allow fixation of radioactive iodide.

Iodine-125 is produced in nuclear reactor from Xenon-124. It decays by electron capture and internal conversion to Tellurium-125. Photons of 27.4 keV, 31.0 keV and 35.5 keV (average 29 keV) are emitted. Its half-life is 59.43 days (KAPLAN, 1978). The primary radioactive iodine solution, in the form of sodium iodide (NaI^{125}), was acquired from Isotop- Russia with 37 GBq (1 Ci), diluted in NaOH solution, pH 8–10, in small volumes (about 0.9 mL). The NaI is completely soluble under the experiment conditions - solubility of sodium iodide in water, 184 g/100 mL at 25 °C with pH between 8 and 9.5. The fabrication route used was not provided by the supplier (probably due to industrial secret. A copy of the certificate can be found in SI).

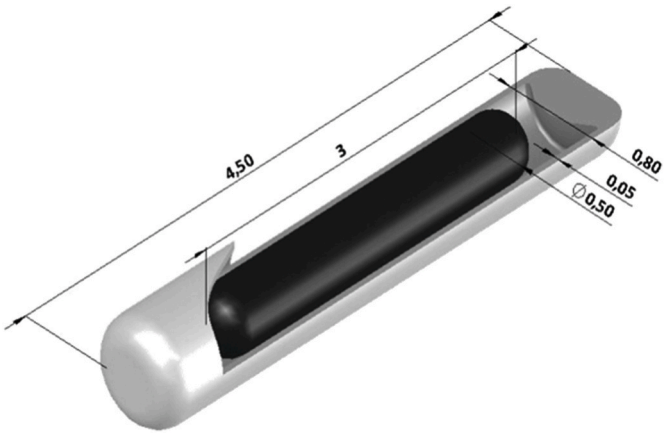

Fig. 1. Schematics of iodine seed. It consists of a silver core that has the iodine-125 deposited onto the surface and a titanium capsule. Dimensions in mm.

2.1. Binding reaction

In a typical experiment, 3 modified cores are placed in a 0.5 mL vial containing 12 μL of radioactive solution and 88 μL of deionized water. The reaction is maintained under stirring (by a rotating reactor) overnight. The cores are removed from the vial and their radioactivity is measured by a Capintec 15R ionization chamber. The final yield is calculated by direct measurement of the core, as follows (eq. (1)). The reason why the efficiency was calculated in this manner and the procedure used for the measurement are found in SI:

$$\text{total yield}_{\%} = \frac{\text{Total activity}_{\text{beginning}}}{\sum \text{Cores}_{\text{after 24h}}} * 100 \quad (1)$$

All tests were performed in triplicate and an average efficiency was calculated and presented as the final result. Since reaction with the unmodified silver core yielded only 8.00% ± 0.57%, surface modification reaction is performed in order to achieve a higher yield.

2.2. Core modification reaction

The core modification reaction was performed by placing the silver cores into pure sodium thiosulfate powder reactant (Fisher Scientific, catalog number S47412, with 99% purity USP grade). We use the jewelry patina process as an inspiration. Basically, to darken a silver piece, jewelers used a sodium thiosulfate solution. Then to do the details on the piece, they "clean it" with a sodium iodine solution (Hughes and Rowe, 1982). The chemical reaction involved is (eq. (2)):

$$2Ag^+ + S_2O_3^{2-} \rightarrow Ag_2(S_2O_3) + 2NaI \rightarrow 2AgI \quad + 2Na^+ \quad + \quad S_2O_3^{2-} \quad (2)$$

One hundred of the untreated silver cores were placed in 10 g of pure sodium thiosulfate. They took 7 days to completely blacken. After this process they were ready to use. Cores maintain viable usage for over one year.

2.3. Optimization of reaction parameters for iodination

The photo-sensibility, reaction vial type, the substitution for iodine-131, pH, and solution volume were evaluated as a possible variable.

Iodine salts and solutions are advised to be stored in dark bottles due to the fact that iodine reacts with light and undergo a photo decomposition reaction (Royal Chemical Society, 2015). Although performing a radioactive reaction in the absence of light is impractical, we wanted to accessed how much would impact iodine yield. This was only performed after extensive practice with the use of an indirect handheld red light was used.

Eight different storage vials were tested by Kennedy et al.(Kennedy and Besses, 1967) in regards to its ability to contain iodine-131 during 24 h. Fig. 2a show the results from the study. Glass yielded the best results, with 10% loss and polyethylene the worse with >50% loss. In this work, eight different reaction vials were also tested.

He et al.(He et al., 2009) evaluate the Iodine-125 activity intake on silver cores by varying the value of pH. They have found that the intake in the silver cores were higher at a low pH (Fig. 2b). The authors affirm that if pH is kept high, the $Na^{125}I$ solution will remain stable not releasing the $^{125}I^-$ for silver binding. In the present wok, three pH values were tested: 1.6.1 (final reaction pH without pH adjustment), and 10. One millimolar solution of NaOH (Synth, analytic purity grade, micropearls) and HCl (ProQuímicos, analytic purity grade, 37%) were used to adjust pH.

Reaction volume was also tested to investigate any relation with efficiency due to its direct correlation with solution concentration and air area available inside the reaction vial.

Since many researchers report their results using iodine-131 stating they will have the same results with iodine-125, (thus solving measurements errors and iodine-125 fabrication difficulties), we repeated

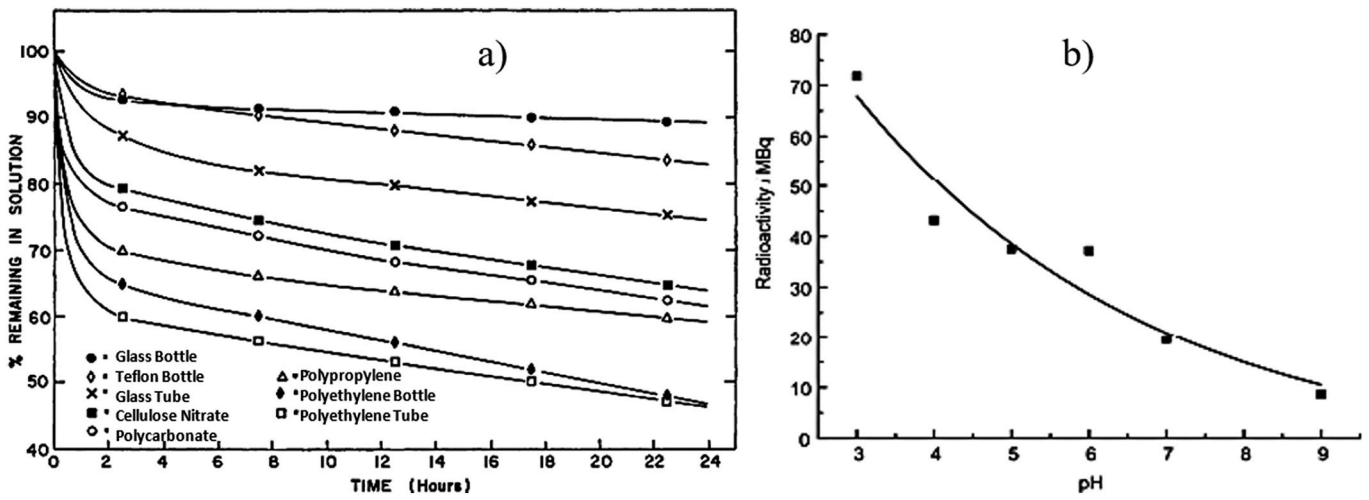

Fig. 2. a) Percentage of radioactive iodine remaining in solution for different materials per hour. "Reprinted with permission from Kennedy et al.(Kennedy and Besses, 1967) Copyright (2019) Journal of Nuclear Medicine". b) Iodine-125 activity intake on silver cores by value of pH. "Reprinted with permission from He et al. (He et al., 2009) Copyright (2019) Nuclear Science and Technology".

our reaction testing if the substitution is valid.

2.4. Surface modification evaluation

The surface modification was evaluated by scanning electron microscopy (SEM) and by Energy Dispersive X-ray Spectroscopy (EDS) FEI Quanta 250 (Inkson, 2016; Leng, 2013). Fourier-Transform Infra-red spectroscopy (FTIR) Agilent Technologies Cary 600 FTIR Spectrometer was also performed for identification (Petit and Madejova, 2013; Reusch, 2013; Ye and Spencer, 2017). Since there are no carbon bounds, only the fingerprint region will be presented. Sulfur peaks of interest are presented in figure caption and sodium thiosulfate structure is presented in Fig. 3. Bare silver spectra will be used for comparison.

2.5. Monte Carlo simulation

Monte Carlo simulation was performed to evaluate the TG-43 (Rivard et al., 2004) parameters for this source using the MCNP6 transport code. Dose to water, D_w, was considered according to the protocol. The seed was modeled with the same geometry presented (Fig. 1). Iodine-125 was considered to be homogeneously distributed in the surface of the silver core. The medium was a 15 cm radius sphere of pure water. The source photons output was previously evaluated and recorded on a phase space file, thus guaranteeing the actual run a homogeneous medium. The seed end was modeled as ellipsoids following measurements over microscopic images of the weld. A homemade routine in MATLAB® was programmed to retrieve the TG-43 parameters from the output of the MCNP run. Details on how seed welding is made can be found on SI.

3. Results

3.1. Iodine-125 reaction

Table 1 presents the results for the final iodine-125 intake in the

Table 1
Iodine-125 intake for the sodium thiosulfate treated silver core.

	Sodium Thiosulfate Treated Silver Core		
	Run 1	Run 2	Run 3
Total Activ.- MBq (mCi)	112.5 (3.04)	111 (3.00)	129 (3.49)
Silver 1- MBq (mCi)	31.70 (0.856)	28.34 (0.766)	34.33 (0.928)
Silver 2- MBq (mCi)	29.41 (0.795)	22.26 (0.601)	26.82 (0.725)
Silver 3- MBq (mCi)	24.53 (0.663)	22.48 (0.607)	33.21 (0.897)
Total- MBq (mCi)	85.64 (2.31)	73.08 (1.97)	94.36 (2.55)
Yield %	76.12	65.84	73.15
Average Yield % (Mean ± SD)	71.70 ± 5.30		

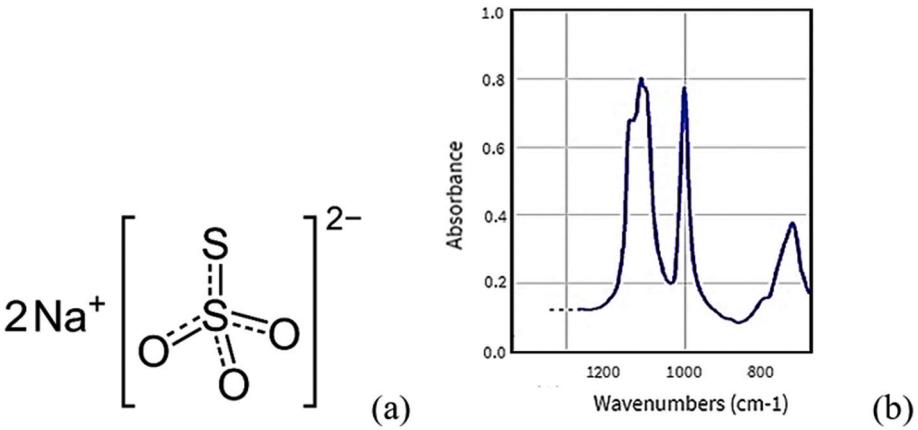

Fig. 3. a) sodium thiosulfate structure, b) IR spectra for sodium thiosulfate, fingerprint region. Double peak in ≈1180-1110 cm^{-1}, subsequent single peak ≈1000 cm^{-1}, and final peak ≈650 cm^{-1} (Liu et al., 2017; National Center for Biotechnology Information, PubChem Compound Database; NIST, 2018).

silver core. The yield percentage was calculated by equation (1).

3.2. Photo-sensibility

Silver Halogens (F, Cl, Br, I) are extremely photo-sensitive materials largely used as photographic emulsions. They absorb the light that hits them generating electrons easily donated Ag^{+} sites. Then, metallic silver is form and the halogen combine with other halogen forming a gaseous molecule that ends up being emitted (Yu et al., 2012).

To access light influence, a reaction was performed in the absence of light with the use of an indirect handheld red light. The efficiency results were: 69.79% ± 7.80 in the presence of light and 83.09% ± 3.30 without the presence of light. Since there is a small statistical difference, the manufacture laboratory will be constructed with minimal direct light as possible.

3.3. Reaction vial

The reaction was performed in 8 different vials with different sizes and materials to access if that was an impact on the final yield (Fig. 4). Results are in Table 2.

Although the statistical difference between the activity vials are small, the one chosen considered availability and practicality. Vial a is heat shut being impossible to be implemented in a manufacture routine. Vial b,c, f, and g are not largely available in our laboratory. Vial d yielded the lower results. Vial h is a $Na^{125}I$ commercialization vial produced specifically by/for the manufacturer. And vial e gave the largest yields value and is largely available.

This effect probably occurs due to iodide (I^{-}) adsorption on the vials. Adsorption is the adhesion of atoms, ions or molecules from a gas, liquid or dissolved solid to a surface (Miessler et al., 2013). All the bonding necessities (ionic, covalent, or metallic) of the constituent atoms of a given material are filled by other atoms in the material. But the atoms on the surface are not wholly surrounded therefore are able to attract adsorbates. This problem is well known with radioactive iodine, specially iodine-131. Imarisio et al. (Imarisio and Greco, 1964) noticed the issue during in vitro testing with small quantities of iodine-131 and even stated that iodine binding is a significant factor. Iodine have such high adsorption rate that is even used to measure the surface area of carbon blocks (Puri and Bansal, 1965).

3.4. The substitution for iodine-131

Some authors use iodine-131 instead 125 due to easy access/production (Puchalska and Mielcarski, 2003; Rostelato, 2006). Both "iodines" (NaI^{125} and NaI^{131}) used are fabricated in a nuclear reactor, however they are purified and prepared differently. That means the reactants used in the process were different and/or different concentrations. Also, 370 MBq (1 mCi) of each isotope result in a different number of atoms:

(continued on next column)

Table 2
Average efficiency of 3 runs for each vial.

	Average Efficiency %
a	68.05 ± 7.50
b	53.20 ± 9.00
c	51.09 ± 8.79
d	54.65 ± 2.52
e	71.70 ± 5.30
f	52.96 ± 4.87
g	62.36 ± 7.69
h	62.54 ± 2.82

(continued)

To iodine-131:
Half-life: 8.04 days

$$A = \lambda \cdot N$$

$$10^{-3} \cdot 3.7 \cdot 10^{10} = \frac{\ln 2}{8.04 \cdot 24 \cdot 60 \cdot 60} \cdot N$$

$$N = 3.70 \cdot 10^{13} \ atoms \ in \ 1 \ mCi$$

$$m = 8.06 \cdot 10^{-9} g \ in \ 1 \ mCi$$

To iodine-125:
Half-life: 59.43 days

$$A = \lambda \cdot N$$

$$10^{-3} \cdot 3.7 \cdot 10^{10} = \frac{\ln 2}{59.43 \cdot 24 \cdot 60 \cdot 60} \cdot N$$

$$N = 2.70 \cdot 10^{14} atoms \ in \ 1 \ mCi$$

$$m = 5.75 \cdot 10^{-8} \ g \ in \ 1 \ mCi$$

Were A being activity in Becquerel, λ is the decay constant, and N is the Avogadro Number. The results were: for NaI^{131} = 28.04% ± 8.75 and for NaI^{125} = 71.07% ± 6.07. Even if the production methods were exactly the same, the reaction reactants proportions should be different for each isotope. Since a very small number of radioactive atoms are being used, every little impurity becomes a massive problem. For instance, if the supplier changes a reactant brand in the purification process, the impurities will change, and the entire process may be affected.

Also, iodine-131 has an energy emission 10 times larger than iodine-125 (364 KeV and 29 KeV, respectively) which implies in better precision in activity measurement.

3.5. pH

Experiments were performed from acid (pH = 1) to basic (pH = 10) range. Those values were achieved by adding drops of HCl and NaOH from solutions with 1 mM until the desired pH was achieved. Also, a reaction without any pH corrections was performed (pH was naturally 6.10 when no modifications were made). The average efficiency values were: for pH 1, 53.39% ± 9.07; for pH 6.1, 71.70% ± 5.30; and for pH 10, 59.33% ± 5.04.

There was a significant difference among yields achieved by distinct pH values implying that one unmodified, close to neutral (pH 6.1) achieved the perfect balance between iodine volatilization (avoided by high pH) and iodide available in the solution (stimulated by low pH).

3.6. Solution volume

The solution volume was tested to access if could impact yield. The silver cores have a small surface area (21.20 mm^3) that in reaction was

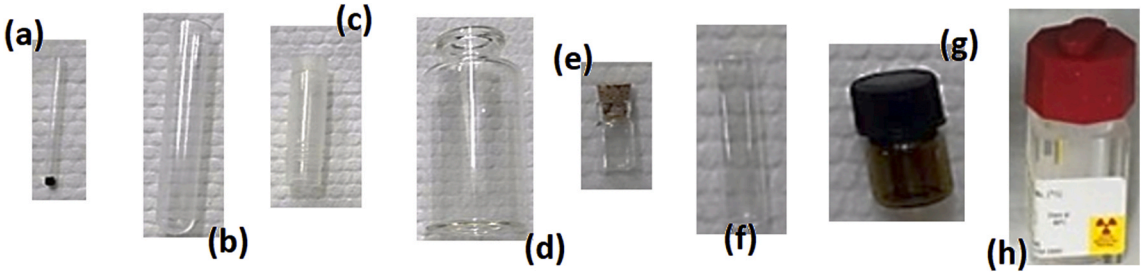

Fig. 4. Vials used to perform the iodine-125 fixation reaction (a) Borosilicate glass tube heat welded in both sides; (b) Poly (methyl methacrylate) tube; (c) Polystyrene tube; (d) Regular glass vial 1; (e) Borosilicate glass vial; (f) Regular glass vial 2; (g) Ambar glass vial; (h) Vial used in the commercialization of $Na^{125}I$.

observed to be even smaller because cores tend to rotate agglomerated (as shown in Fig. 5). Also, in small volumes the solution would present higher concentration (radioactive iodine/volume), that could result in more iodide (I^-) finding its way to silver cations (Ag^+) forming the desired $Ag^{125}I$. At the opposite, a lower air quantity inside the reaction vial could result in less evaporation, thus less iodide loss. Results were: for 100 μL with 666 KBq/μL (0.018 mCi/μL), 71.70% ± 5.30, and for 500 μL with 133 KBq/μL (0.0036 mCi/μL), 53.82% ± 7.02. This indicates that lower reaction volumes can result in higher yields.

3.7. Surface analysis

Fig. 6 presents the FT-IR graph. Coinciding peaks from the silver core treated with sodium thiosulfate and pure sodium thiosulfate reagent are shown. Fig. 7 shows EDS analysis confirming the presence of sulfur in the treated core surface.

Figs. 6 and 7 Results shows that surface modification was achieved. SEM images of bare silver and the sodium thiosulfate modification silver are presented in Figs. 8 and 9.

Fig. 8 shows that the bare silver is etched, probably from fabrication machinery. Fig. 9 shows the surface modification after the treatment. Apparently, thiosulfate plaques are formed in the surface. Since a SEM image of the radioactive core is not possible, an evaluation if the iodide bounds to sulfur or silver is not able to be made (AgI or Ag_3IS may form in the surface. They have very close structural relationship (Perenthaler et al., 1981)). This, however can greatly impact dose distribution.

3.8. Monte Carlo study

A total of 3.5×10^7 number of particle-stories were simulated. Statistical uncertainty for all values presented are within ±3%, except for $\theta = 0°$, where $\sigma > 5\%$ only for the points r = 5 cm, r = 7 cm and r = 10 cm, due to low photon income because of both the weld and distance of the source. The calculated value for the dose-rate constant was $\Lambda = 0.829 \pm 0.005$ cm^{-2}, which is lower than other well-established commercial iodine-125 seeds, indicating a steep dose gradient. Table 3 show: the results for radial dose function and anisotropy functions, respectively, at some specific radii; and the parameters for the fifth-order polynomial fitting for g(r) as suggested by TG-43 protocol, up to r = 15 cm with a 0.5 cm step. Parameters a0 through a5 fit the data within ±1%, which agree with the 2% agreement proposed by the protocol. Fig. 10 presents the plot for g(r) in all points evaluated and the respective fit curve. Fig. 11 presents plots and Table 4 the values for F (r,θ) at some radii, in all evaluated angles. The values for low angles at higher radii are expected, as the anisotropy shall fall with increasing distance up to a distance far enough so the source can be considered a point source.

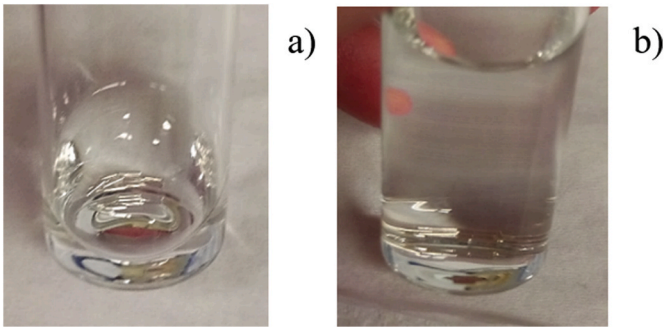

Fig. 5. Photos representing the position of the silver cores inside the reaction vial a) vial containing 1 mL of solution, b) vial containing 5 mL of solution. Agitation was performed by a rotating reactor.

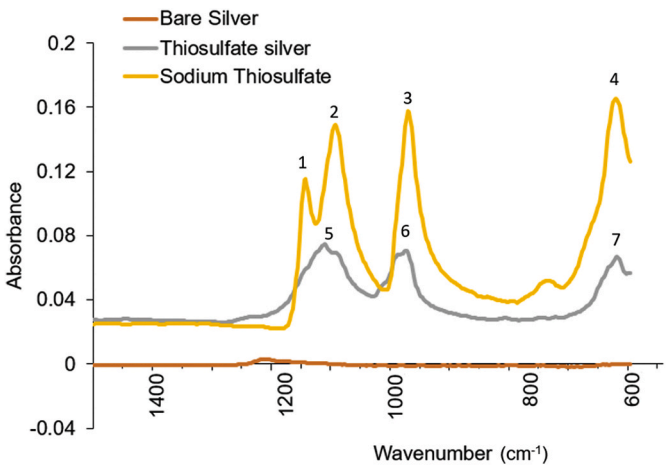

Fig. 6. FTIR spectra of untreated (bare) silver core, treated thiosulfate silver core and pure sodium thiosulfate reactant. Sodium thiosulfate reagent (yellow curve): (1) (2) duplet in 1160 cm^{-1} and 1114 cm^{-1} (3) 995 cm^{-1} (4) 653 cm^{-1}; Silver core treated with sodium thiosulfate (grey curve): (5) duplet 1130 and 1114 cm^{-1} (6) 995 cm^{-1} (7) 657 cm^{-1}. Untreated silver core (orange curve) showed no signal, as expected. (For interpretation of the references to colour in this figure legend, the reader is referred to the Web version of this article.)

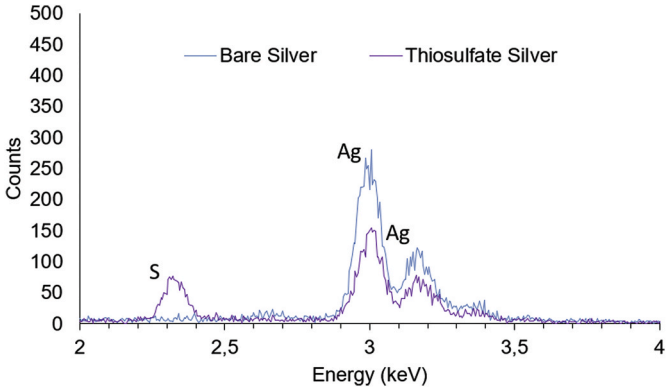

Fig. 7. EDS analysis. Results confirm the presence of sulfur in the treated core.

4. Discussion and conclusion

In order to reduce costs and provide treatment for more Brazilians, IPEN is building a laboratory for the manufacture of radioactive sources for brachytherapy treatment. In order to develop the new seed, a thorough study was performed, not only considering the important radiochemical aspects but also the manufacture process demands. This paper presented a new methodology for fixating the I^{125} onto silver core based on thiosulfate-iodide exchange reaction that presented a 71.70% yield. Studies are being made in order to access if the remaining 29.30% can be reused.

Several parameters were evaluated. They were chosen based on the radiochemical characteristics, literature discrepancy in calculations, and issues encountered during the realization of the experiments. The difference in the photo-sensibility study, 13.3%, is considerable. However, implementing a radioactive manufacturing process in total absence of light is unfeasible. But knowing its relevancy, impacted the way we are building our laboratory (with as low direct light incidence as possible). The vial used in the reaction has proven to be a minor yield influencer. The vial chosen for our manuterge process presented the highest yield and is largely available. The reaction pH value had a direct impact on the reaction yield. The best result was achieved by maintaining pH value slightly acidic (6.1). Since the silver cores remains

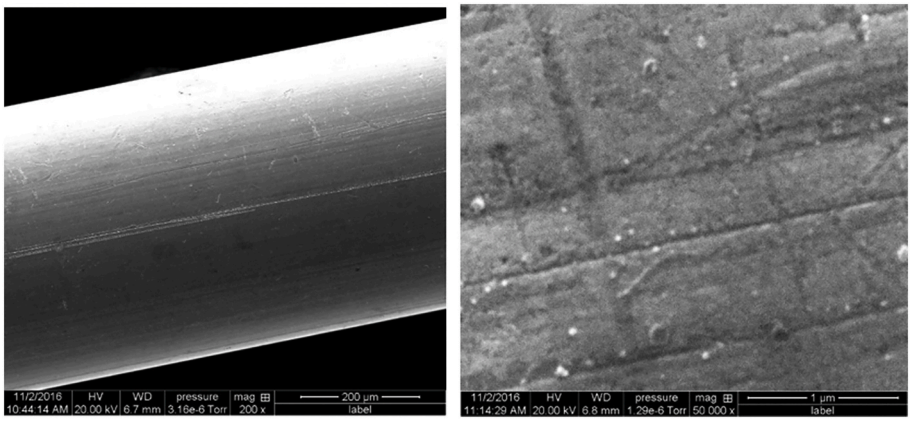

Fig. 8. SEM image of bare silver. Magnification of 200 and 1 μm.

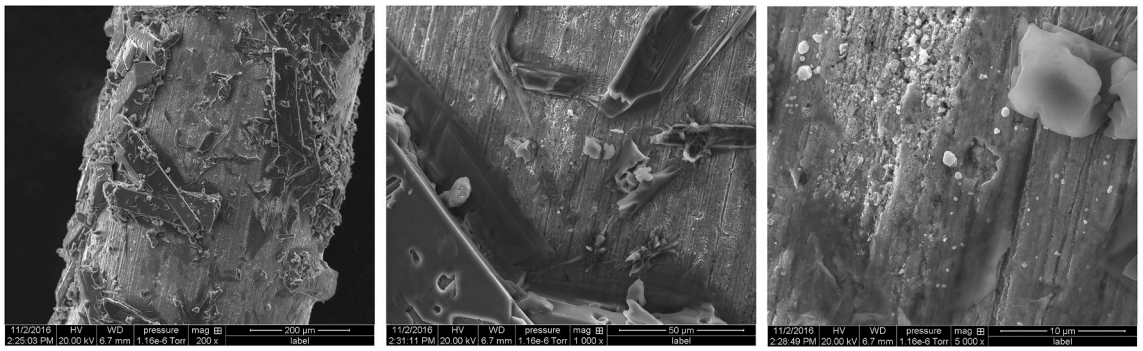

Fig. 9. SEM image of thiosulfate silver. Magnification of 200, 50, and 10 μm. Core modification is clearly shown. Attention to the uneven structures (≈200 μm) in the surface.

Table 3
Values for radial dose function, g(r), calculated with MCNP6 code and Values for the fitting parameters for g(r) as a 5th order polynomial.

Radial Dose Function g(r)		Fitting Parameters for g(r)	
R	g(r)	Fitting Parameters	Values
0.5	1.063	a_0	1.146
1	1.000	a_1	-1.384×10^{-1}
1.5	0.917	a_2	1.950×10^{-2}
2	0.830	a_3	4.845×10^{-3}
2.5	0.742	a_4	-3.352×10^{-4}
3	0.659	a_5	7.833×10^{-6}
4	0.507		
5	0.386		
7	0.216		
10	0.087		

agglomerated at the end of the vial diminishing even less the binding surface available, large reaction volumes should be avoided. The more concentrated, thus less volume, more iodine-125 will reach the silver active sites, binding into it.

The surface modification analysis showed the treatment with sodium thiosulfate made an impact on the surface. Although the attribution of functions for FT-IR peaks in the fingerprint region is a difficult and, sometimes, not accurate, a comparison analysis between the modifying agent, the bare sample and the modified sample can be considered valid (Answered by Prof. Ernest Z. from Acadia University, 2016; Leng, 2013; Reusch, 2013; Ye and Spencer, 2017). The sulfur that came from sodium thiosulfate was also found in EDS. SEM of the treated cores showed that an uneven ≈200 μm rectangular structures were formed in the surface. They are probably plaques of thiosulfate that has deposited and that will latter chemically exchange with iodine-125.

The MCNP simulation output follows the expected result. The radial dose function shows the dose decay due to scattering and absorption in the medium with the distance of the center of the source, in the transverse plane, thus ignoring the dose fall by geometric conditions. Considering only this aspect, the dose is expected to be half the reference point value at 4 cm away, which represents a steep dose gradient; at 5 cm, the contribution from both the geometry function and dose radial function shows that the delivered dose is only one tenth the reference point value. The anisotropy function also follows the expected result, with a smooth fall at lower angles except by a steep fall around 0°, which is result of the higher thickness of the welds. It is also expected that its effect is less pronounceable at higher distances.

To complete master the production our group have successfully manufactured iodine-125 at IPEN's nuclear reactor in an attempt to control all the possible variables. Good Manufacturing Processes evaluation are being performed. The evaluation of iodine-125 binding site and if the uneven structures in the treated core affect dosimetry will be evaluated in future work.

Declaration of competing interest

No conflict of interest.

CRediT authorship contribution statement

Carla Daruich de Souza: Conceptualization, Data curation, Formal analysis, Investigation, Methodology, Project administration, Validation, Visualization, Writing - original draft, Writing - review & editing. **Carlos Alberto Zeituni:** Funding acquisition, Project administration, Resources, Supervision, Validation, Visualization. **Anselmo Feher:** Data curation, Formal analysis, Writing - review & editing. **João Augusto**

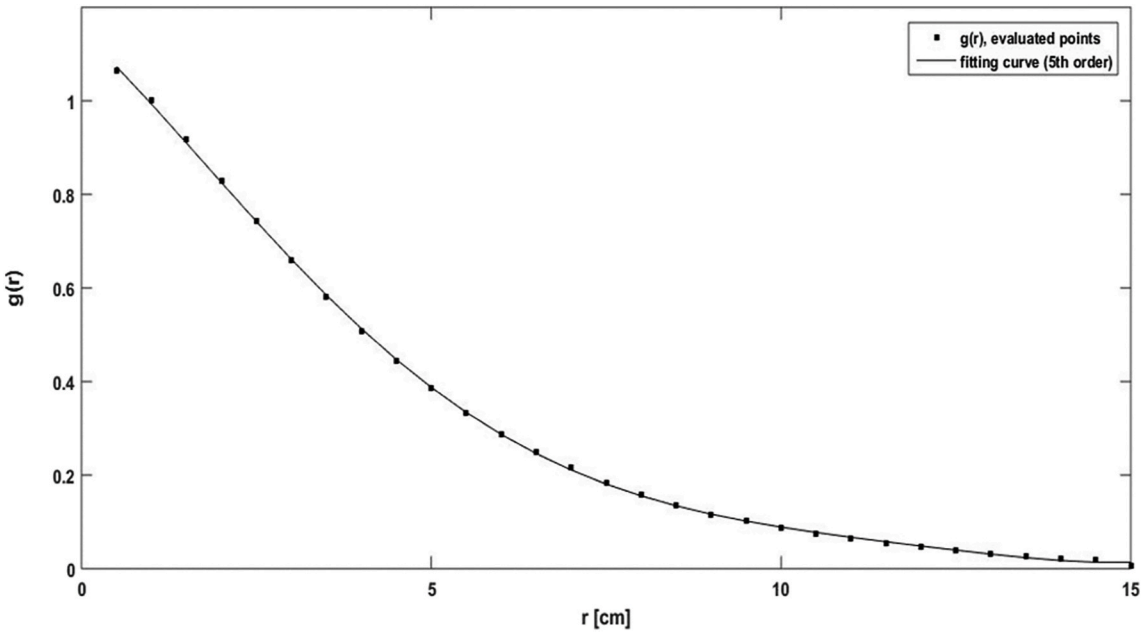

Fig. 10. Plot for g(r) evaluated points and fitting polynomial curve.

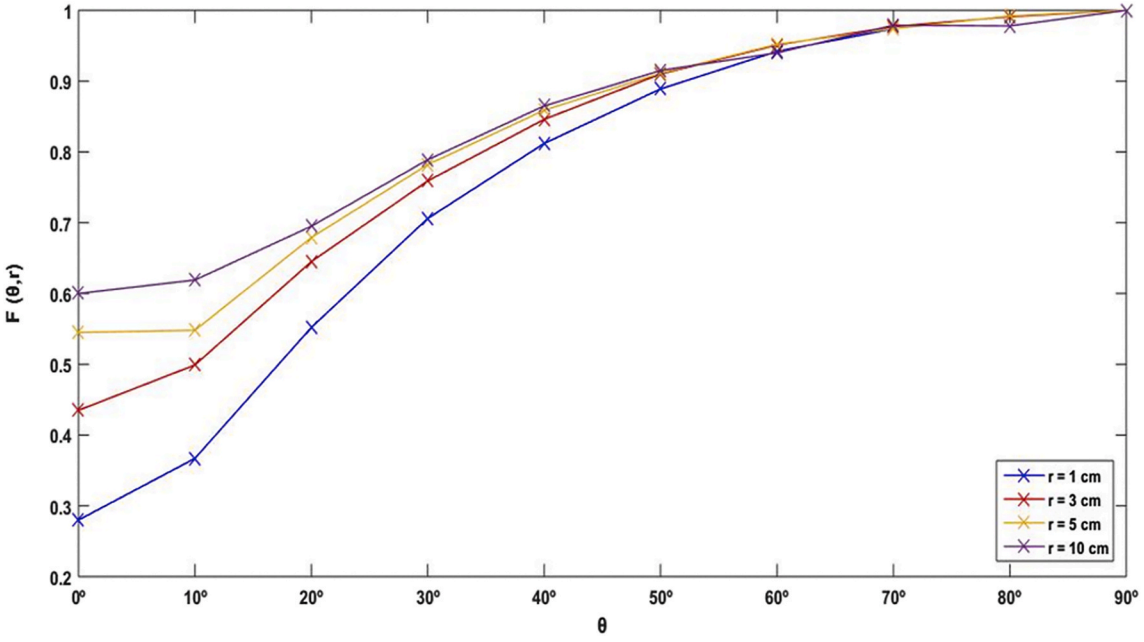

Fig. 11. Plot for F (θ,r) for values up to 90° and radii of 1, 3, 5 and 10 cm.

Table 4
Values for anisotropy function, F (r,θ), calculated with MCNP6 code.

	r									
θ	**0.5**	**1**	**1.5**	**2**	**2.5**	**3**	**4**	**5**	**7**	**10**
0°	0.201	0.280	0.325	0.362	0.414	0.435	0.464	0.545	0.460	0.600
10°	0.303	0.367	0.417	0.454	0.479	0.499	0.529	0.548	0.590	0.619
20°	0.474	0.552	0.593	0.616	0.631	0.645	0.670	0.679	0.697	0.695
30°	0.661	0.706	0.726	0.740	0.753	0.759	0.773	0.782	0.791	0.789
40°	0.795	0.812	0.826	0.835	0.840	0.846	0.853	0.859	0.867	0.865
50°	0.878	0.889	0.898	0.903	0.906	0.910	0.913	0.911	0.916	0.915
60°	0.933	0.942	0.946	0.948	0.949	0.951	0.958	0.952	0.952	0.940
70°	0.969	0.974	0.978	0.977	0.978	0.977	0.981	0.974	0.982	0.979
80°	0.991	0.992	0.994	0.994	0.994	0.991	0.996	0.992	0.989	0.978

Moura: Supervision, Writing - review & editing. **Osvaldo Luiz da Costa:** Supervision, Writing - review & editing. **Lucas Verdi Angelocci:** Conceptualization, Data curation, Formal analysis, Software, Validation, Visualization, Writing - original draft, Writing - review & editing. **Maria Elisa C.M. Rostelato:** Formal analysis, Funding acquisition, Project administration, Resources, Supervision, Validation.

Acknowledgments

This work was supported by IAEA- International Atomic Energy Agency for granting fellowship [BRA16021]; and CAPES – Coordenação de Aperfeiçoamento de Pessoal de Nível Superior. CDS would like to thank: Dr. Paul D. Benny, Dr. Thomas R. Hayes, and Washington State University for academic support; Dr. Marc-André Fortin and Dr. Pascale Chevallier of Université Laval.

Appendix A. Supplementary data

Supplementary data to this article can be found online at https://doi.org/10.1016/j.apradiso.2020.109307.

References

Answered by Prof. Ernest Z. from Acadia University, 2016. Topic discussion: how can I distinguish functional group region and fingerprint region in a infrared spectrum? https://socratic.org/questions/how-can-i-distinguish-functional-group-region-and-fingerprint-region-in-a-infrar.

Cardoso, R.M., de Souza, C.D., Rostelato, M.E.C.M., Araki, K., 2017. Highly efficient method for production of radioactive silver seed cores for brachytherapy. Appl. Radiat. Isot. 120, 76–81.

Chodak, G., 2014. Prostate brachytherapy has good long-term outcomes. Medscape. https://www.medscape.com/viewarticle/833145.

Cutrer, L.M., 1999. Laser Welded Brachytherapy Source and Method of Making the Same in: North American Scientific.

Cutrer, L.M., 2003. Radioactive seed with multiple markers and method for using same. In: North American Scientific.

Goldner, G., Pötter, R., Battermann, J.J., Schmid, M.P., Kirisits, C., Sljivic, S., van Vulpen, M., 2012. Comparison of seed brachytherapy or external beam radiotherapy (70 Gy or 74 Gy) in 919 low-risk prostate cancer patients. Strahlenther. Onkol. 188, 305–310.

He, J.H., Jiang, L., Xingliang, L., Wenbin, Z., Jing, W., Zongping, M., Yuan, J., 2009. Preparation of the radioactive source core of iodine-125 seed. Nucl. Sci. Tech. 20, 231–234.

Hughes, R., Rowe, M., 1982. The Colouring, Bronzing and Patination of Metals. Crafts Council, EUA.

Imarisio, J.J., Greco, J., 1964. Glass binding of labeled thyroxine and triiodothyronine. Biochim. Biophys. Acta Gen. Subj. 82, 172–175.

Inkson, B.J., 2016. 2 - scanning electron microscopy (SEM) and transmission electron microscopy (TEM) for materials characterization. Materials Characterization Using Nondestructive Evaluation (NDE) Methods. Woodhead Publishing, pp. 17–43.

International Atomic Energy Agency, 2006. Production Techniques and Quality Control of Sealed Radioactive Sources of Palladium-103, Iodine-125, Iridium-192 and Ytterbium-169 (TECDOC-1512) (Viena).

Kaplan, I., 1978. Física Nuclear, vol. 2. Guanabara Dois, Rio de Janeiro, RJ.

Kennedy, J.A., Besses, G.S., 1967. Comparison of adsorption of iodine-131-thyroxine to glass and plastic containers. J. Nucl. Med. 8, 226–228.

Kubiatowicz, D.O., 1982. Radioactive Iodine Seed. MINNESOTA MINING AND MANUFACTURING COMPANY.

Lawrence, D.C., 1967. Therapeutic metal seed containing within a radioactive isotope disposed on a carrier and method of manufacture. In: Hazleton Nuclear Science Corporation.

Leng, Y., 2013. Materials Characterization: Introduction to Microscopic and Spectroscopic Methods, 2 ed. Wiley - VCH.

Liu, C., Wang, C., Li, Y., Rao, Z., 2017. Preparation and characterization of sodium thiosulfate pentahydrate/silica microencapsulated phase change material for thermal energy storage. RSC Adv. 7, 7238–7249.

Mellor, J.W., 1965. A Comprehensive Treatise on Inorganic and Theoretical Chemistry. Longmans, Green and CO, Londres.

Miessler, G.L., Fischer, P.J., Tarr, D.A., 2013. Inorganic Chemistry. Prentice Hall, EUA.

Ministério da Saúde. Instituto Nacional de Câncer, 2018. Incidência de Câncer no brasil. http://www.inca.gov.br/estimativa/2018/estimativa-2018.pdf.

National Center for Biotechnology Information. PubChem Compound Database Sodium Thiosulfate. https://pubchem.ncbi.nlm.nih.gov/compound/Sodium_thiosulphate#section=Top.

NIST, 2018. Sodium Thiosulfate. http://webbook.nist.gov/cgi/cbook.cgi?ID=B6000554&Mask=80.

Perenthaler, E., Schulz, H., Beyeler, H.U., 1981. Structures and phase transition of [beta]- and [gamma]-Ag3IS. Acta Crystallogr. B37, 7.

Petit, S., Madejova, J., 2013. Chapter 2.7 - fourier transform infrared spectroscopy. In: Faïza, B., Gerhard, L. (Eds.), Developments in Clay Science. Elsevier, pp. 213–231.

Puchalska, I., Mielcarski, M., 2003. Seed-less iodine-125 ophthalmic applicator. Appl. Radiat. Isot. : including data, instrumentation and methods for use in agriculture, industry and medicine 58, 15–20.

Puri, B.R., Bansal, R.C., 1965. Iodine adsorption method for measuring surface area of carbon blacks. Carbon 3, 227–230.

Reusch, W., 2013. Infrared Spectroscopy. https://www2.chemistry.msu.edu/faculty/reusch/virttxtjml/spectrpy/infrared/infrared.htm.

Rivard, M.J., Coursey, B.M., DeWerd, L.A., Hanson, W.F., Huq, M.S., Ibbott, G.S., Mitch, M.G., Nath, R., Williamson, J.F., 2004. Update of AAPM Task Group No. 43 Report: a revised AAPM protocol for brachytherapy dose calculations. AAPM-American Association of Physics in Medicine 42. https://www.aapm.org/pubs/reports/rpt_84.pdf.

Rostelato, M.E.C.M., 2006. Estudo e Desenvolvimento de uma nova Metodologia para Confecção de Sementes de Iodo-125 para Aplicação em Braquiterapia. Instituto de Pesquisas Energéticas e Nucleares, IPEN-CNEN/SP, São Paulo.

Royal Chemical Society, 2015. Iodine. http://www.rsc.org/periodic-table/element/53/iodine.

Russel, J., 2004. A century of brachytherapy. Nucl. News 47, 44–46.

Souza, C.D., 2009. Braquiterapia com sementes de Iodo-125: manufatura e tratamento. Universidade Estadual Paulista, Instituto de Biociências, Botucatu, São Paulo.

Souza, C.D., 2012. Comparação entre métodos de fixação do iodo radioativo em substrato de prata para confecção de fontes utilizadas em Braquiterapia. Instituto de Pesquisas Energéticas e Nucleares, IPEN-CNEN/SP, São Paulo.

Suthanthiran, K., Lakshman, R., 1991. Pellet for a radioactive seed. In: Best Industries.

Ye, Q., Spencer, P., 2017. 9 - analyses of material-tissue interfaces by Fourier transform infrared, Raman spectroscopy, and chemometrics. In: Material-Tissue Interfacial Phenomena. Woodhead Publishing, pp. 231–251.

Yu, H., Liu, L., Wang, X., Wang, P., Yu, J., Wang, Y., 2012. The dependence of photocatalytic activity and photoinduced self-stability of photosensitive AgI nanoparticles. Dalton Trans. 41, 10405–10411.

Zeituni, C.A., Souza, C.D., Moura, E.S., Sakuraba, R.K., Rostelato, M.E.C.M., Feher, A.M., Somessari, S.L., Costa, O.L., 2012. Theoretical, manufacturing and clinical application aspects of a prostate brachytherapy I-125 source in Brazil. In: Kishi, K. (Ed.), BRACHYTHERAPY. InTech, Rijeka, Croácia, p. 17.